

# Nonlinear Model for Offline Correction of Pulmonary Waveform Generators

Jeffrey S. Reynolds\*, *Member, IEEE*, Kimberly J. Stemple, Raymond A. Petsko, Thomas R. Ebeling, and David G. Frazer

**Abstract**—Pulmonary waveform generators consisting of motor-driven piston pumps are frequently used to test respiratory-function equipment such as spirometers and peak expiratory flow (PEF) meters. Gas compression within these generators can produce significant distortion of the output flow–time profile. A nonlinear model of the generator was developed along with a method to compensate for gas compression when testing pulmonary function equipment. The model and correction procedure were tested on an Assess Full Range PEF meter and a Micro DiaryCard PEF meter. The tests were performed using the 26 American Thoracic Society standard flow–time waveforms as the target flow profiles. Without correction, the pump loaded with the higher resistance Assess meter resulted in ten waveforms having a mean square error (MSE) higher than  $0.001 \text{ L}^2/\text{s}^2$ . Correction of the pump for these ten waveforms resulted in a mean decrease in MSE of 87.0%. When loaded with the Micro DiaryCard meter, the uncorrected pump outputs included six waveforms with MSE higher than  $0.001 \text{ L}^2/\text{s}^2$ . Pump corrections for these six waveforms resulted in a mean decrease in MSE of 58.4%.

**Index Terms**—American Thoracic Society (ATS), gas compression, nonlinear, pump, waveform generator.

## I. INTRODUCTION

THE use of computer-controlled mechanical syringes (waveform generators) for testing spirometers and peak flow meters is common [1]–[4]. The American Thoracic Society (ATS) recommends a set of 24 volume–time waveforms [5] and a set of 26 flow–time waveforms [6] for testing pulmonary function equipment. When testing equipment with very low flow resistance, waveform generators have little difficulty producing these waveforms accurately. However, gas compression within the pump (or syringe) system can create significant errors when testing higher resistance devices, or when using waveforms with fast rise times.

Navajas *et al.* [7] investigated compression effects in waveform generators when testing peak expiratory flow (PEF) meters. Significant errors were reported when generating waveforms with large initial pump chamber volumes. They proposed an empirical approach to correcting for gas compression, relying only on truncated scaled versions of standard

volume–time waveform 24. This approach was supported by a simple description of the pump, which was modeled as a time-invariant low-pass filter. No attempt was made to correct the waveform generator to deliver the ATS standard waveform profiles accurately.

Hankinson *et al.* [8] solved the distortion problem with the use of an adaptive algorithm for generating a pump input that accurately delivers the desired waveform. A significant contribution of this paper was a method to calculate nozzle flow based on piston displacement and pump chamber pressure. This method alleviates the need for a pneumotach, which can add significantly to gas compression. The adaptive algorithm in [8] is online, where the pump must deliver a waveform at each iteration in the adaptive process. A model of the pump system is not presented.

Miller *et al.* [9] suggest that errors in pump systems are due to wave action rather than gas compression. They use a calculation of Mach number in the pump nozzle as a basis for an incompressible flow model. However, the model does not account for the increase in static pressure in the pump chamber, where the gas is compressed due to force exerted by the pump piston. Here the air is unable to escape the chamber in a timely manner due to the restriction presented by the pump nozzle and load. Additionally, if the air inside the pump acted as an incompressible fluid, the flow at the pump output could simply be taken as the flow calculated via movement of the piston. There would be no need to model the system or measure the pressure inside the pump chamber.

We developed an alternate technique of correcting the pump input to produce the ATS standard waveforms. Using a nonlinear model of the pump system, a method of offline input correction was developed that allows accurate waveform delivery at the output of the generator.

## II. METHODS

### A. Equipment

The system used to generate pulmonary waveforms was identical to the one described by Hankinson, *et al.* [8] (Fig. 1). A commercially available computer controlled mechanical syringe<sup>1</sup> was used to deliver the ATS waveforms. The pump nozzle on the faceplate had a slight bevel in the transition region of the flat plate and the nozzle. The radius of curvature of the bevel was approximately 0.14 times the nozzle diameter in order to minimize the energy loss associated with the change in diameter [10]. Custom software installed on a personal computer

Manuscript received September 5, 2001; revised July 9, 2002. Asterisk indicates corresponding author.

\*J. S. Reynolds is with the Engineering and Controls Technology Branch, Health Effects Laboratory Division, National Institute for Occupational Safety and Health, Morgantown, WV 26505 USA (e-mail: JReynolds@cdc.gov).

T. R. Ebeling, and D. G. Frazer are with the Engineering and Controls Technology Branch, Health Effects Laboratory Division, National Institute for Occupational Safety and Health, Morgantown, WV 26505 USA.

K. J. Stemple and R. A. Petsko are with the Field Studies Branch, Division of Respiratory Disease Studies, National Institute for Occupational Safety and Health, Morgantown, WV 26505 USA.

Digital Object Identifier 10.1109/TBME.2002.805484

<sup>1</sup>MH Custom Design, Midvale, UT.

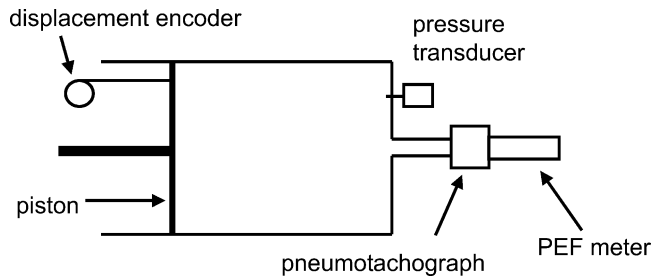


Fig. 1. System diagram. The pneumotachometer was used for model validation and removed during testing.

(PC 486 32 MHz) was used to control the pump and acquire measurements. Pump pressure was measured using a capacitive pressure transducer.<sup>2</sup> For validation of nozzle flow calculation, flow through the pump nozzle was measured with a pneumotachometer<sup>3</sup> connected to a pressure transducer.<sup>4</sup> Both the pressure and the flow signals were passed through analog two pole antialiasing filters with cutoffs of 150 Hz. These signals were then routed to a simultaneous sample and hold board<sup>5</sup> connected to a data acquisition card<sup>6</sup> in the PC. Piston displacement was measured by sampling a digital rotary encoder signal (which reflects motor shaft rotation) routed from the manufacturers motor control card to a quadrature encoder input board.<sup>7</sup> The accuracy of this signal was verified by comparison to an encoder attached directly to the piston, thus reflecting linear motion. All signals were sampled at a frequency of 2000 Hz. Input waveforms were delivered to the mechanical pump at a rate of 500 Hz.

The pneumotach was calibrated by delivering 35 constant flow waveforms (Fig. 2), each having a volume of 12 liters (L). The flows ranged from 0.8 L/s to 14.4 L/s in 0.4 L/s increments. For each waveform, a calibration factor multiplied by the integral of the pneumotach signal was set equal to 12 L. A curve fit was applied to these data yielding an expression for flow as a function of raw "counts" ( $y = 0.016x$ ).

The pump pressure transducer was calibrated with a u-tube manometer. Since the linearity of the pressure transducer was within 0.1% full scale, a simple span calibration was all that was required. An ambient pressure signal was first recorded. A pressure of 20 cm of red oil (specific gravity = 0.826) was then applied, and a reading recorded. The difference of these two recordings divided by the applied pressure (adjusted for the specific gravity of the red oil) produced the static pressure gain applied to the raw pressure readings.

### B. Output Flow Calculation

Although a pneumotach can be used to measure pump flow directly, this increases the system flow resistance. Since gas compression in the pump is related to system flow resistance, the pneumotach increases the likelihood that compression will affect any particular waveform. By choosing an approach to eliminate this added resistance, we likely decrease the number of

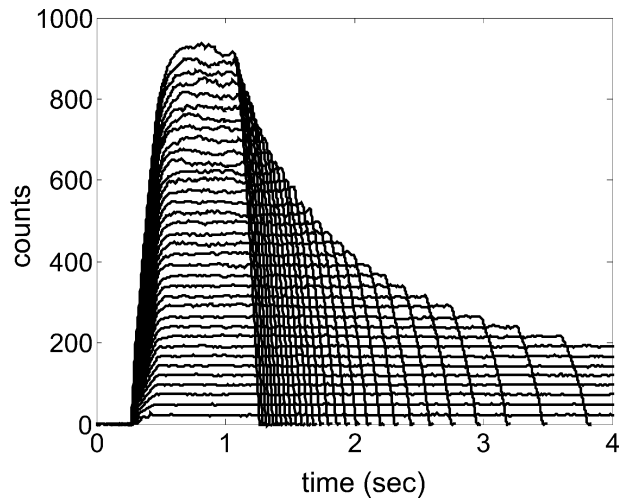


Fig. 2. Set of 35 flow waveforms recorded with a pneumotachometer for calibration. The steady portions of these waveforms correspond to flows from 0.5 L/s to 14.4 L/s in 0.4 L/s increments.

ATS waveforms that might otherwise require correction when testing PEF meters. Additionally, small deviations in placement of the pneumotach produced marked changes in the calibration curve. Therefore, the method of [8] was used to calculate pump output flow.

Briefly, the volume of gas compressed as a function of time,  $v_c(t)$  can be expressed as

$$v_c(t) = v_s(t) \left[ \left( \frac{p_s(t)}{P_B} \right)^{1/\gamma} - 1 \right] \quad (1)$$

where  $v_s(t)$  is the instantaneous syringe volume,  $p_s(t)$  is the instantaneous syringe pressure,  $P_B$  is barometric pressure, and  $\gamma$  is the ratio of molar heat capacity at a constant pressure to the molar heat capacity at a constant volume (for air,  $\gamma = 1.4$ ). Numerical differentiation of (1) yields compressive flow  $f_c(t)$ . Total output flow  $f_o(t)$  is then described as the difference between flow produced by displacement of the piston,  $f_d(t)$ , and the compressive flow

$$f_o(t) = f_d(t) - f_c(t). \quad (2)$$

The pneumotach was used to verify the accuracy of (1) and (2). The pneumotach and PEF meter were attached to the pump nozzle. ATS flow waveforms 22, 25, and 26 were delivered three times each, and the output flow calculated for each waveform. These output flows were then compared to the calibrated pneumotach signals to validate this technique. Fig. 3 shows the results of this quality control procedure using waveform 25. Similar results were obtained with all three waveforms. The MSE between the pneumotach flow and the calculated flow was then evaluated

$$\text{MSE} = \frac{1}{N} \sum_{i=1}^N (f_p(i) - f_o(i))^2 \quad (3)$$

where  $f_p(i)$  represents pneumotach flow,  $f_o(i)$  the calculated flow, and  $N$  the total number of samples. The average MSE for

<sup>2</sup>Setra Systems model 239, Acton, MA.

<sup>3</sup>Hans Rudolph model 3813, Kansas City, MO.

<sup>4</sup>Micro Switch model 176PC14HD2, Freeport, IL.

<sup>5</sup>Keithley-Metrabyte model SSH-8, Taunton, MA.

<sup>6</sup>Keithley-Metrabyte model DAS-1800, Taunton, MA.

<sup>7</sup>Keithley-Metrabyte model M5312, Taunton, MA.

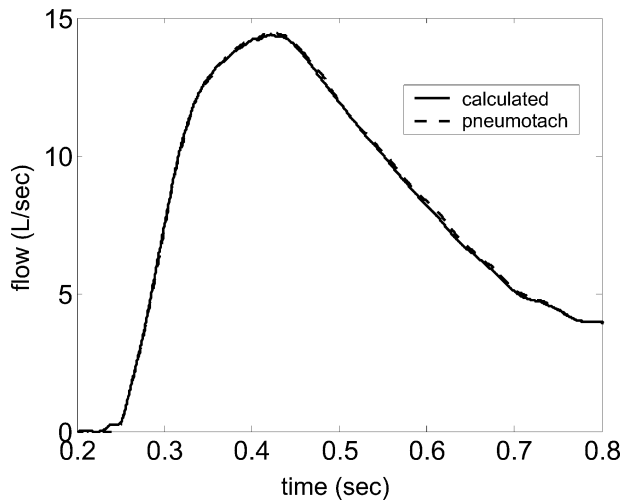


Fig. 3. Comparison of waveform generator output flow measured by pneumotach and output flow calculated from piston displacement and pump pressure. The calculated flow was taken as the true output flow in this study.

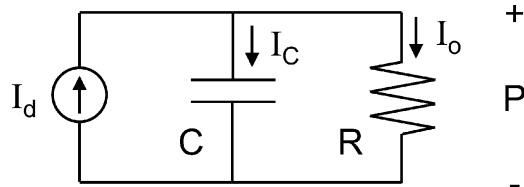


Fig. 4. Circuit model used to describe the pulmonary waveform generator with resistive load.

waveforms 22, 25, and 26 were 0.000925, 0.00200, and 0.00187  $L^2/s^2$ , respectively.

### C. Generator Model

The pump system with load (PEF meter attached to the pump nozzle) was modeled as a parallel combination of a compliant element and a resistive element. The compliant element represents gas compressibility within the pump chamber. The resistive element represents the flow impedance of the load. The electric circuit analog is shown in Fig. 4, where voltage, current, electrical resistance, and capacitance are analogous to pressure, volumetric flow, flow resistance, and gas compliance, respectively. The current  $I_d$  represents the flow produced by displacement of the pump piston. The current  $I_c$  represents the portion of this flow “lost” to gas compression or “gained” from gas rarefaction. The current  $I_o$  is the resulting flow out through the load, and the voltage  $P$  represents the pressure generated within the pump chamber.

The flow produced by movement of the piston is equal to the sum of the output flow and the compressive flow (a positive compressive flow indicates gas compressed, while a negative value indicates gas expanded)

$$I_d(t) = I_o(t) + I_c(t). \quad (4)$$

The resistance of the load is, in general, a nonlinear function of the flow through the load. Therefore, the output flow is written

$$I_o(t) = \frac{P(t)}{R(I_o(t))}. \quad (5)$$

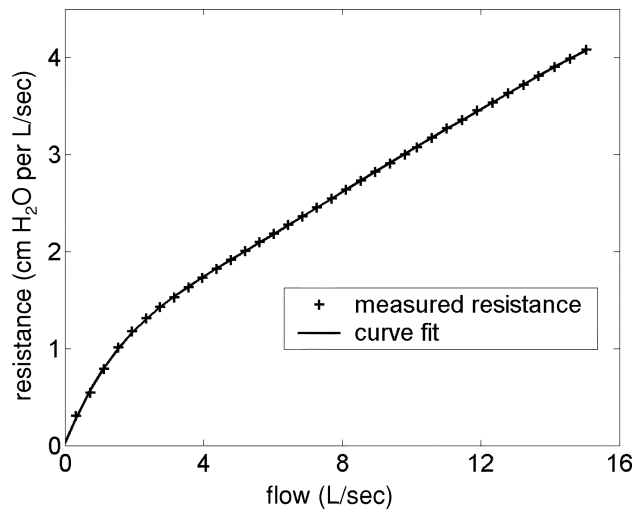


Fig. 5. Flow resistance of Load A as a function of the flow through Load A.

Additionally, the pump volume changes with the stroke of the piston. Since gas compliance is a function of volume, the compliant element acts as a time-varying capacitor. The compressive flow is then

$$I_c(t) = \frac{d}{dt} [C(v(t)) \cdot P(t)] \quad (6)$$

where  $v(t)$  is pump volume. Combining (4)–(6) gives

$$I_d(t) = I_o(t) + \frac{d}{dt} [R(I_o(t)) \cdot C(v(t)) \cdot I_o(t)]. \quad (7)$$

The nonparametric system descriptions  $R(f)$  and  $C(v)$  were determined experimentally. Resistance as a general function of flow,  $R(f)$  was determined in a manner similar to the pneumotach calibration. A number of static flows were produced through the load, resulting in corresponding constant pressure profiles within the pump. For each static flow profile, resistance was taken as mean pressure divided by mean flow. Each value of resistance was plotted versus mean flow, and a polynomial curve fit applied (Fig. 5). This resulted in a general expression for  $R(f)$  which could be evaluated at any desired flow–time profile  $f = I_o(t)$ .

Integrating both sides of (6) and solving for  $C(t)$  gives

$$C(t) = \frac{\int I_c(t)}{P(t)} = \frac{v_c(t)}{P(t)} \quad (8)$$

where  $v_c(t)$  is the volume compressed. Pump compliance was found by delivering one of the ATS waveforms and measuring pump pressure and piston displacement. Evaluation of (1) and (8) yielded  $C(t)$ . A plot of  $C(t)$  versus time is shown in Fig. 6.  $C(t)$  was then plotted versus pump volume, and a curve fit applied. This produces the desired expression for  $C(v)$ , which can be evaluated at any desired volume–time profile  $v = v(t)$ , provided the system remains isentropic. Note that the choice of waveforms for calculation of  $C(v)$  is not critical. However, it is recommended that the waveform have a fast rise time (maximum signal to noise ratio of the pump pressure signal) and a large volume (the curve fit is applied across a larger span of the independent variable). We chose the ATS flow–time waveform 25 (rise time = 57.9 ms, volume = 6.38 L). Also, since the

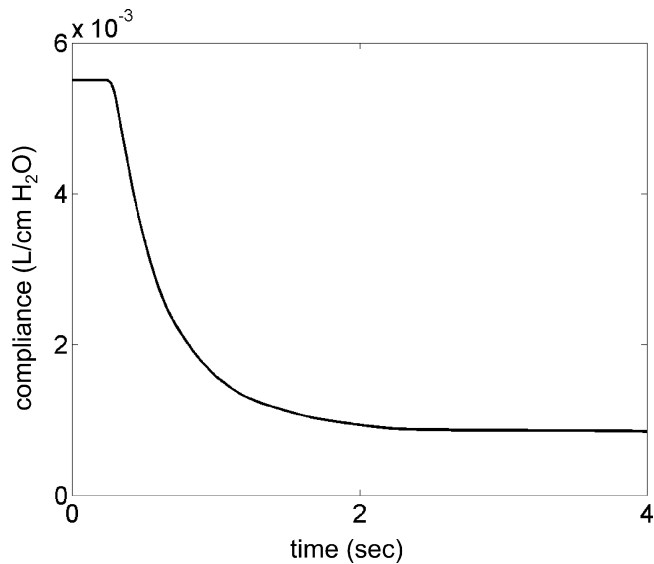


Fig. 6. Pump chamber gas compliance, as a function of time, during delivery of ATS standard flow-time waveform 25.

volume of gas compressed in the pump is a function of barometric pressure [see (1)], the pump compliance in our model is affected by changes in atmospheric conditions. However, these errors are quite small, and were, therefore, neglected.

#### D. Pump Input Correction

In order to solve (7) for a piston motion profile  $I_d(t)$  that produces a desired output flow  $I_o(t)$ ,  $R(f)$ , and  $C(v)$  must be evaluated for the specific profile. Let the constant  $v_{total}$  be the initial volume of the pump prior to delivery of a waveform. In our system,  $v_{total}$  was minimized for each waveform by withdrawing the piston just enough to deliver the necessary volume. As the piston moves forward during the stroke, the pump volume is decreased. The pump volume as a function of time during delivery of a given waveform is

$$v(t) = v_{total} - \int I_d(t) \cdot dt. \quad (9)$$

Evaluating  $R(f)$  at  $f = I_o(t)$  and  $C(v)$  at  $v = v(t)$ , (7) can be rewritten as

$$I_d(t) = I_o(t) + \frac{d}{dt} \cdot \left[ R(I_o(t)) \cdot C \left( v_{total} - \int I_d(t) \cdot dt \right) \cdot I_o(t) \right]. \quad (10)$$

A nonlinear least squares routine that utilized a Gauss-Newton gradient search algorithm [11] was used to solve (10) for  $I_d(t)$ . Note that  $R(I_o(t))$  can be calculated *a priori*, while  $C(v(t))$  must be recalculated at each iteration as  $I_d(t)$  is adapted.

#### E. Experimental Protocol

The offline pump correction scheme was tested using two loads: Load A, an Assess Full Range meter,<sup>8</sup> and Load B, a Micro DiaryCard meter.<sup>9</sup> We chose to test with the ATS standard

<sup>8</sup>Health Scan Products Inc., Cedar Grove, NJ.

<sup>9</sup>Micro Direct Inc. model MD01, Lewiston, ME.

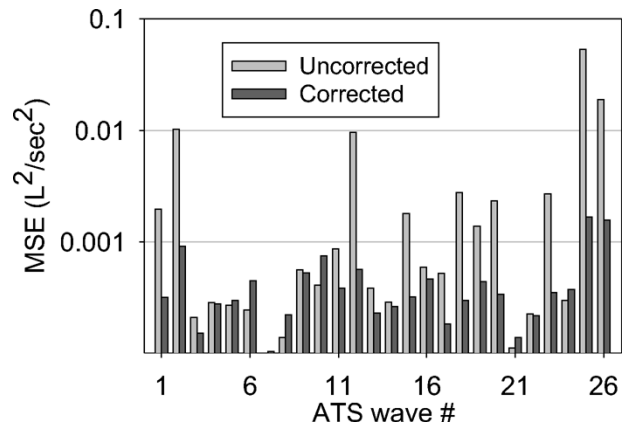


Fig. 7. MSE (from target to delivered) for the 26 ATS standard flow-time waveforms delivered by the pulmonary waveform generator with Load A at the generator output.

flow-time waveforms. These waveforms have faster rise times than the ATS standard volume-time waveforms and would be likely to produce more compression in the pump chamber than the volume-time profiles. The original ATS waveforms, representing the target flow profiles, were delivered three times each and the output flows, or uncorrected flow profiles, were calculated. The corrected pump inputs were then delivered three times each and the output flows, or corrected flow profiles, were calculated.

In order to evaluate the total distortion between the target waveforms and delivered waveforms, the MSE was calculated. Note that delivered waveforms refers to the output flow calculated via (2). Misalignment between the input and output signals is a result of delay in the software and motor control card and phase shift due to the filtering effect of gas compression. Since we were not concerned with the time at which the waveform was sent, but only the shape of the waveform, the input and output signals had to be aligned. The signals were aligned by computing the cross correlation function between target and delivered flow signals. The time index at which the maximum of the cross correlation occurred was taken as the shift between signals. The signals were then pre- or postzero padded as needed to align and equalize lengths. The MSE was then calculated

$$MSE = \frac{1}{N} \sum_{i=1}^N (y_t(i) - y_d(i))^2 \quad (11)$$

where  $y_t(i)$  represents target flow,  $y_d(i)$  the delivered flow, and  $N$  the total number of samples.

### III. RESULTS

Results for Load A are shown in Fig. 7. Ten uncorrected waveforms had MSEs greater than  $0.001 \text{ L}^2/\text{s}^2$ . Correction of inputs for these ten waveforms resulted in an average MSE reduction ( $\pm$  standard error) of  $87.0(\pm 2.70)\%$ . Correction of inputs for the remaining 16 waveforms resulted in an average MSE increase of  $3.91(\pm 11.4)\%$ .

Fig. 8 illustrates the results for ATS standard waveform 10 using Load A. The MSE for the uncorrected output is  $0.00040 \text{ L}^2/\text{s}^2$ . The MSE for the corrected output is  $0.00075 \text{ L}^2/\text{s}^2$ . Although the corrected waveform has a greater MSE (85% higher)

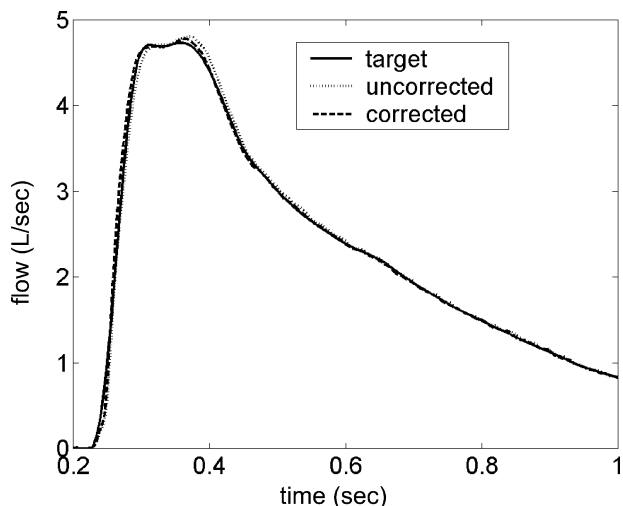


Fig. 8. Pump output flow for ATS flow-time waveform 10 (Load A). This is an example of a waveform with uncorrected MSE less than  $0.001 \text{ L}^2/\text{s}^2$ . In this case, the corrected waveform MSE is actually 85% higher than the uncorrected, while neither waveform exhibits large deviations from target flow.

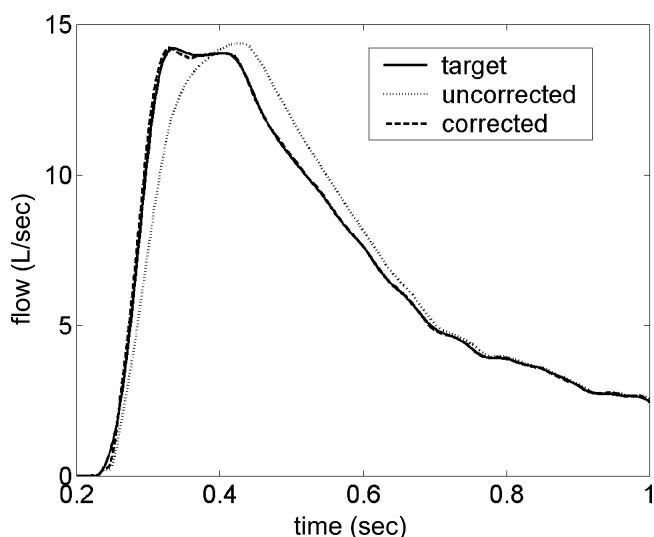


Fig. 9. Pump output flow for ATS flow-time waveform 25 (Load A). This is an example of a waveform with uncorrected MSE greater than  $0.001 \text{ L}^2/\text{s}^2$ . Correction for this waveform results in an output flow with a 97% reduction in MSE. Clearly, the uncorrected output flow deviates significantly from the target flow.

than the original, both the uncorrected and the corrected output flows accurately follow the target. In fact, near the peak of the waveform, the corrected waveform is more accurate than the uncorrected.

Fig. 9 illustrates results for ATS standard waveform 25 with Load A. MSE for the uncorrected and corrected outputs are  $0.053$  and  $0.0016 \text{ L}^2/\text{s}^2$ , respectively. Here, correction results in a 97% reduction of the MSE. Clearly, correction of this waveform results in a significant improvement with respect to the target flow.

When testing with Load B at the pump output, six uncorrected waveforms had an MSE greater than  $0.001 \text{ L}^2/\text{s}^2$  (Fig. 10). After correction of these six waveforms, the average MSE was reduced by  $58.4(\pm 7.63)\%$ . Correction of inputs

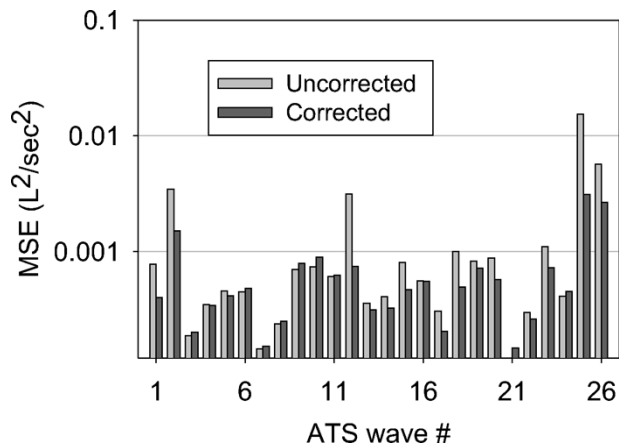


Fig. 10. MSE (from target to delivered) for the 26 ATS standard flow-time waveforms delivered by the pulmonary waveform generator with Load B at the generator output.

for the remaining 20 waveforms resulted in an average MSE reduction of  $6.58(\pm 4.65)\%$ .

Since gas compression in the pump chamber is the primary cause of waveform distortion, one might expect large MSE for waveforms that have larger/faster changes. A parameter that reflects this type of change in pulmonary function testing is the forced expiratory volume in the first second (FEV1). The ten uncorrected waveforms of Load A with MSE greater than  $0.001 \text{ L}^2/\text{s}^2$  correspond to the ATS waveforms with the ten highest FEV1s [6]. The six uncorrected waveforms of Load B with MSE greater than  $0.001 \text{ L}^2/\text{s}^2$  correspond to ATS waveforms with six of the seven highest FEV1s.

#### IV. DISCUSSION

A method for producing accurate representations of the ATS flow-time waveforms using a mechanical pump has been previously reported [8]. That method employed an adaptive algorithm that computed the desired waveform by converging on a suitable solution using a method of steepest descent. The techniques used in this study, however, have several advantages to achieve similar accuracies. First, the new method does not require repetitive pump activity to determine the necessary corrections. As a result, pump wear during a testing period is significantly reduced. Second, the time in which the pump is in use to determine the corrections for improved performance is greatly reduced. This allows more efficient use of the pump since corrections can be determined independently with a stand-alone computer. Third, the mathematical description of the pump, in this study, is based on a lumped parameter physical model composed of discrete components. This allows a more intuitive interpretation of the pump correction process and also has the advantage that the “load” or instrument under test can be characterized in terms of a characteristic impedance. In the past, Navajas *et al.* [7] described a time-invariant model of the pump composed of a simple resistance capacitance network to approximate the filtering effects of gas compression during PEF meter testing. The model described in this study is similar but employs time varying components to more accurately depict the nonlinear nature of the pump system.

It can be shown that the airflow in a pipe of constant cross section is associated with a dynamic pressure term which remains small for Mach numbers less than 0.3. Since these are normally the conditions when using a mechanical pumping system, it would be expected that air flowing in the pump nozzle could be treated as an incompressible fluid. Miller *et al.* [9] recently asserted, for this reason, that all the air in the pump nozzle and chamber can be considered incompressible, and that pressure variations within the system are due to acoustical vibration. We believe, however, that even though the air velocity is lower in the pump chamber, and the dynamic terms are negligible, large compressional forces can be exerted on the gas within the pump chamber. The static pressure developed in the pump chamber caused by the restriction of the pump nozzle and "load" can reach total pressures appreciably higher than atmospheric pressure and, therefore, must be considered.

It should also be noted that, although we did not find it necessary to include an electrical representation of the dynamics of the pump servo control system, it could have been added. When the pump was in operation, the servo system provided displacement feedback to a motor control card to ensure that the pump piston followed the correct position with respect to time and generated the desired trajectory.

When testing PEF meters using the ATS waveforms, it might seem reasonable to be concerned only with the accurate reproduction of the correct peak flow. It has been shown, however, that a variety of curve shapes and/or rise times with similar peak flows are necessary to insure the accuracy of a given PEF meter [6]. The use of waveforms having differing flow-time characteristics is an indirect method of evaluating the frequency response of a device. The overall frequency characteristics of the meter under test affects how well peak flow is estimated under a variety of flow-time conditions. The ATS has specified accuracy recommendations for pump systems [12] based on selected parameters such as PEF and forced expiratory FEV<sub>1</sub>. We believe, however, that the mean square error between the actual flow delivered and the desired flow signal is a more meaningful index of the pump's ability to accurately deliver the desired ATS waveforms. This type of analysis answers questions concerning the pump's performance, in terms of waveform reproduction that incorporates the frequency response of the system.

In order to evaluate the performance of both the pulmonary waveform generator and the correction procedure, an accurate measurement of output flow is required. Two obvious choices are a pneumotach and a previously described method [8] based on piston displacement. Like most measurement systems, various corrections may be applied to achieve increased accuracy. While using a differential pressure type pneumotach, corrections can be made for gas composition, gas density, and temperature, as well as frequency-response compensation. Likewise, the piston displacement method uses pump chamber pressure to correct for gas compression. Although either technique could be used to measure the output flow, we chose to use the piston displacement method due to the problems associated with using a pneumotach inline with the PEF meter

during testing (see Section II-B). We did validate the accuracy of this method, however, by not only relying on [8], but by performing our own experimentation demonstrating the agreement of this method with the flow measured using a pneumotach (see Fig. 3).

Finally, it should be noted that the model described in this paper was tested with a pump loaded with two different devices. Each device was accurately described by a purely resistive element. Since PEF meters are generally small and contain only a small amount of dead space, this is normally the case. If one considers the bandwidth represented by the 26 ATS standard waveforms, however, devices having excessive dead space, length, or moving parts may require a model having additional capacitive and/or inductive elements to adequately describe the dynamic characteristics of the load. Under these more complicated conditions, the load impedance becomes a function of frequency as well as flow.

In summary, this study shows that a pump system and load can be accurately described by a model comprised of time varying components. Application of the model in performing offline corrections to account for gas compression errors results in an improved delivery of the ATS standard waveforms for testing and calibrating devices that are used to evaluate pulmonary flow-volume parameters. Examples shown in this study indicate that flow-time profiles having mean square errors with respect to the desired waveform that are greater than 0.001 L<sup>2</sup>/s<sup>2</sup> can be significantly improved by the described correction procedure.

## REFERENCES

- [1] S. B. Nelson, R. M. Gardner, R. O. Crapo, and R. L. Jensen, "Performance evaluation of contemporary spirometers," *Chest*, vol. 97, no. 2, pp. 288-297, 1990.
- [2] R. M. Gardner, R. O. Crapo, B. R. Jackson, and R. L. Jensen, "Evaluation of accuracy and reproducibility of peak flowmeters at 1,400 m," *Chest*, vol. 101, no. 4, pp. 948-952, 1992.
- [3] M. R. Miller, S. A. Dickinson, and D. J. Hitchings, "The accuracy of portable peak flow meters," *Thorax*, vol. 47, no. 11, pp. 904-909, 1992.
- [4] A. C. Jackson, "Accuracy, reproducibility, and variability of portable peak flowmeters," *Chest*, vol. 107, no. 3, pp. 648-651, 1995.
- [5] J. L. Hankinson and R. M. Gardner, "Standard waveforms for spirometer testing," *Amer. Rev. Resp. Dis.*, vol. 126, no. 2, pp. 362-364, 1982.
- [6] J. L. Hankinson and R. O. Crapo, "Standard flow-time waveforms for testing of PEF meters," *Amer. J. Resp. Critic. Care Med.*, vol. 152, no. 2, pp. 696-701, 1995.
- [7] D. Navajas, J. Roca, R. Farre, and M. Rotger, "Gas compression artefacts when testing peak expiratory flow meters with mechanically-driven syringes," *Eur. Resp. J.*, vol. 10, no. 4, pp. 901-904, 1997.
- [8] J. L. Hankinson, J. S. Reynolds, M. K. Das, and J. O. Viola, "Method to produce American Thoracic Society flow-time waveforms using a mechanical pump," *Eur. Resp. J.*, vol. 10, no. 3, pp. 690-694, 1997.
- [9] M. R. Miller, B. Jones, Y. Xu, O. F. Pedersen, and P. H. Quanjer, "Peak expiratory flow profiles delivered by pump systems. Limitations due to wave action," *Amer. J. Resp. Critic. Care Med.*, vol. 161, no. 6, pp. 1887-1896, 2000.
- [10] R. L. Street, G. Z. Watters, and J. K. Vennard, *Elementary Fluid Mechanics*. New York: Wiley, 1996, pp. 363-364.
- [11] T. F. Coleman, M. A. Branch, and A. Grace, *Optimization Toolbox User's Guide*. Natick, MA: The Mathworks, Inc., 1999.
- [12] American Thoracic Society, "Standardization of spirometry: 1994 update," *Amer. J. Resp. Critic. Care Med.*, vol. 152, no. 3, pp. 1107-1136, 1995.



**Jeffrey S. Reynolds** (S'91–M'99) received the B.S. degrees in electrical and computer engineering from West Virginia University, Morgantown, in 1993. He is currently working towards the M.S. degree in electrical engineering from West Virginia University.

He is a registered Professional Engineer in West Virginia, and is currently a Research Engineer at the National Institute for Occupational Safety and Health, Morgantown, WV. His research interests include biomedical signal processing and dynamic system modeling.



**Thomas R. Ebeling** received the B.S. and M.S. degrees in electrical engineering from West Virginia University, Morgantown, in 1975 and 1983, respectively.

Since 1975, he has worked as a Research Engineer at the National Institute for Occupational Safety and Health, Morgantown, WV. His research interests include biomedical instrumentation and electronic circuit design.



**Kimberly J. Stemple** received the A.A.S. degree in medical laboratory technology and the B.A. Regents degree from Fairmont State College, Fairmont, WV, in 1987 and 1995, respectively. She is currently working towards the M.P.H. degree in occupational health from Tulane University, New Orleans, LA.

Since 1997, she has been employed as a Health Scientist at the National Institute for Occupational Safety and Health, Morgantown, WV. Her research interests include developing measurement techniques and instrumentation for occupational health studies.



**Raymond A. Petsko** received an electronics education as a Member of the United States Air Force from 1964 to 1968.

Since 1975, he has worked as an Electronics Engineering Technician and Certified Pulmonary Function Technician at the National Institute for Occupational Safety and Health, Morgantown, WV. His research interests include testing pulmonary function equipment and instrument fabrication.



**David G. Frazer** received the B.S., M.S., and Ph.D. degrees in electrical engineering from Pennsylvania State University, University Park, in 1963, 1965, and 1970, respectively. He received the Ph.D. degree in physiology and biophysics from West Virginia University, Morgantown, in 1974.

He is currently employed by the National Institute for Occupational Safety and Health, Morgantown, WV, and is an Adjunct Professor of electrical engineering and an Adjunct Assistant Professor of physiology at West Virginia University. His research interests include lung mechanics, development of lung function testing methods, aerosol science, and the development of small animal exposure systems.